Probing the Active Site of Acetylcholinesterase by Molecular Dynamics of Its Phosphonate Ester Adducts†

Akos Bencsura,‡ Istvan Y. Enyedy, and Ildiko M. Kovach*

Contribution from the Department of Chemistry, The Catholic University of America, Washington, DC 20064

Received July 20, 1995[⊗]

Abstract: Molecular dynamics (MD) simulations using CHARMM were performed for the solution structures of the pentacoordinate and tetracoordinate P_SC_S and P_RC_S adducts of *Torpedo californica (Tc)* acetylcholinesterase (AChE) formed with 2-(3,3-dimethylbutyl) methylphosphonofluoridate (soman) to assess the molecular origins of stereoselectivity of phosphonylation. MD simulations were also carried out for the P_SC_S transients in soman-inhibited trypsin to evaluate the differences in the mode of operation of the two enzymes. Parameters for the pentacoordinate phosphonate fragments were constructed from results of an *ab initio* calculation at the 6-31*G** level for a model compound, and those for the tetracoordinate phosphonate fragments were from MNDO calculations. Starting equilibrium structures for the above and for analogous structures for chymotrypsin were generated and energy-optimized in program YETI. The stereoselectivity of AChE for the levorotatory diastereomers of soman amounts to >5.6 kcal/mol difference in transition state free energies and can be rationalized based on the results of the MD calculations: There is a predominant conformation of transient forms of the P_SC_S diastereomer of soman-inhibited AChE in which every ligand in phosphorus is stabilized by an optimal binding feature of the active site. In contrast, the phosphonyl fragment in the P_RC_S diastereomer may be accommodated with equal difficulty, at least, two different ways: In the most favorable conformation, the phosphoryl oxygen is engaged in weak interactions with constituents of the oxyanion hole if adjustments in the Cα backbone and substantial motions of Trp84, Trp233, Phe288, and Phe290 are allowed. The remarkable efficiency of F^- departure from the pentacoordinate transition states of phosphonylated AChE cannot be explained by general base catalysis by $HisH^+440$. Leaving group departure from these structures must be promoted by electrostatic forces, "push" from Glu199 and "pull" from the oxyanion hole, in addition to steric strain. One of the distinguishing features of the crystal structure of *Tc*AChE is the *short H-bonds in the catalytic triad*. The His440 Nδ---OOCβ Asp327 bond distance is 2.5 Å (2.8 Å resolution) in AChE and 0.2 Å shorter than the corresponding H-bond in trypsin and chymotrypsin (1.5 Å resolution). This distance increased to 2.7 Å during the dynamics simulation. However, the average H-bond distances are further shortened by 0.05−0.3 Å in energy-minimized structures of the adducts of AChE covalently modified by soman at the pentacoordinate and tetracoordinate intermediate stage. MD simulations of the optimized structures of native AChE and its adducts gave insight into how the skeletal motions accommodate an overcrowded active site particularly in the pentacoordinate adducts. The steric relief is only partial and is balanced by a repositioning of Glu199 toward the catalytic triad and phosphonyl fragment. This subtle reorientation of active-site residues should be relevant to the prominent catalytic efficiency of AChE.

Phosphonylation of the active-site serine of hydrolase enzymes presents a variety of questions in mechanistic chemistry that fascinated investigators for decades. Of all serine hydrolase phosphonylations the most consequential is that of acetylcholinesterase (AChE). The recent availability of the X-ray structure[1] of *Torpedo californica* (*Tc*) AChE opened new opportunities for the interpretation of these reactions in structural and atomic detail.[2−12] Serine phosphonylation probably occurs by an in-line displacement of the leaving group and with the intervention of a pentacoordinate transient.[7,13,14] The lifetime of the transient depends on the electronic and steric nature of all substituents not only the leaving group.

† Initial results of this research were presented as an invited contribution titled "Interactions in Tetravalent and Pentavalent Phosphonate Esters of Ser at the Active Site of Serine Enzymes" in a symposium on Antibodies at the XIII International Conference on Phosphorus Chemistry, Jerusalem, Israel, July 16−21, 1995.

‡ On leave from the Central Research Institute for Chemistry of the Hungarian Academy of Sciences, P.O. Box 17 H-1525 Budapest, Hungary.

⊗ Abstract published in *Advance ACS Abstracts,* August 15, 1996.

(1) Sussman, J. L.; Harel, M.; Frolow, F.; Oefner, C.; Goldman, A.; Toker, L.; Silman, I. *Science* **1991**, *253*, 872−879.

(2) Taylor, P.; Radic, Z. *Annu. Rev. Pharmacol. Toxicol.* **1994**, *34*, 281−320.

(3) Tan, R. C.; Truong, T. N.; McCammon, J. A.; Sussman, J. L. *Biochemistry* **1993**, *32*, 401−403.

(4) Cygler, M.; Schrag, J. D.; Sussman, J. L.; Harel, M.; Silman, I.; Gentry, M. K.; Doctor, B. P. *Protein Sci.* **1993**, *2*, 366−382.

(5) Antosiewicz, J.; McCammon, J. A.; Wlodek, S. T.; Gilson, M. K. *Biochemistry* **1995**, *34*, 4211−4219.

(6) Qian, N.; Kovach, I. M. *FEBS Lett.* **1993**, *336*, 263−266.

(7) (a) Bencsura, A.; Enyedy, I.; Kovach, I. M. *Biochemistry* **1995**, *34*, 8989−8999. (b) Enyedy, I.; Bencsura, A.; Kovach, I. M. *Phosphorus, Sulfur and Silicon* **1996**, *109−110*, 249−252.

(8) Kovach, I. M.; Qian, N. F.; Bencsura, A. *FEBS Lett.* **1994**, *349*, 60−64.

(9) Saxena, A.; Qian, N.; Kovach, I. M.; Kozikowski, A. P.; Pang, Y. P.; Vellom, D. C.; Radic, Z.; Quinn, D.; Taylor, P.; Doctor, B. P. *Protein Sci.* **1994**, *3*, 1770−1778.

(10) Ripoll, D. L.; Faerman, C. H.; Axelsen, P. H.; Silman, I.; Sussman, J. L. *Proc. Natl. Acad. Sci. U.S.A.* **1993**, *90*, 5128−5131.

(11) Gilson, M. K.; Straatsma, T. P.; McCammon, J. A.; Ripoll, D. R.; Faerman, C. H.; Axelsen, P. H.; Silman, I.; Sussman, J. L. *Science* **1994**, *263*, 1276−1278.

(12) Axelsen, P. H.; Harel, M.; Silman, I.; Sussman, J. L. *Protein Sci.* **1994**, *3*, 188−197.

(13) Sterri, S. H.; Fonnum, F. *Biochem. Pharmacol.* **1987**, *36*, 3937−3942.

(14) Kovach, I. M. *J. Enzyme Inhib.* **1988**, *2*, 199−208.

S0002-7863(95)02406-1 CCC: $12.00

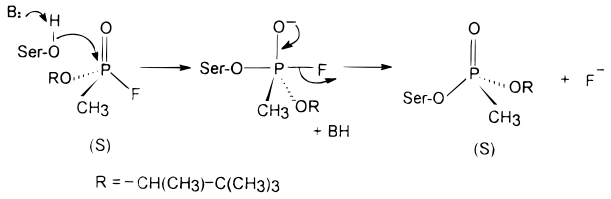

The paradigm of efficient irreversible inhibition of a serine hydrolase is that of AChE by 2-(3,3-dimethylbutyl) methylphosphonofluoridate (soman). The second-order rate constant for the phosphonylation of AChE by soman is $\sim 10^{11}$ times greater than that for the uncatalyzed hydrolysis of soman, while the same comparison for soman inactivation of chymotrypsin and trypsin gives factors of 10^8 and 10^6, respectively.[14−16] The remarkable capacity of AChE for accommodating two of the diastereomers of soman is indeed baffling. Soman differs from the natural substrate, acetylcholine, in that it is uncharged, it has one more ligand at P than the C in carboxyl, and it has a small leaving group in a completely different orientation from active-site-bound choline in acetylcholine. Our previous kinetic studies showed that the rate-limiting process in the inactivation of AChE by soman includes an induced-fit step together with the general base-catalyzed phosphonylation of the active-site Ser.[17,18] We have also demonstrated for the inactivation of AChE with 4-nitrophenyl 2-propyl methylphosphonate that bond breaking to the leaving group is part of the rate-determining process.[18] If this should also be true for soman, a more efficient inhibitor, bond making and breaking would need to be nearly concerted with or preceded by a conformational change.

Serine hydrolase enzymes show stereoselectivity for the levorotatory isomers of soman; $\sim 10^4$ for AChE[19,20] and $\sim 10^2$ for trypsin and chymotrypsin.[21] Based on chemical correlations, the absolute configuration at P(-) was assigned to be S. Chirality at C in the pinacolyl fragment has only a small effect on the rate of phosphonylation.[20,21] If the stereochemical outcome of phosphonylation of the active-site Ser is inversion of configuration, as implied by eq 1, then the P_SC_S diastereomeric adduct of serine hydrolase enzymes would be the product of phosphonylation by the P_SC_S diastereomer of soman.

We have recently reported on molecular mechanics studies of the origins of the dealkylation or aging reaction of soman-inhibited AChE, trypsin, and chymotrypsin.[7,22] The calculations complemented experimental findings and addressed issues inaccessible to experimental observation at this time. Results of the calculation illuminated how useful the tetracoordinate phosphonate esters of the active-site Ser of the enzymes are as transition state analogs for the acylation and deacylation of the enzymes by natural substrates, the role of the acid/base catalytic apparatus, the oxyanion hole, and other polar and nonpolar constituents of the active site in the later phases of the inhibition of the enzymes by organophosphorus compounds. The relative stability of the diastereomeric adducts was also assessed. However, the molecular mechanics calculations were limited to test the motion of side chains and did not permit an evaluation of bonding interactions and motions of the protein backbone: This condition prevented the evaluation of the mobility of catalytic residues in the native and covalently modified enzymes and fosters skepticism about the conclusions on the mode of binding in the diastereomers of the soman-inhibited AChE. The computational study has since been extended to the *initial phases of serine phosphonylation*: It included energy optimization of the diastereomeric pentacoordinate adducts of AChE, trypsin and chymotrypsin with soman followed by the simulation of the dynamics of native AChE and trypsin, the P_SC_S and P_RC_S diastereomers of the soman-inhibited AChE and P_SC_S adduct of soman-inhibited trypsin in the tetracoordinate and pentacoordinate forms. Pentacoordinate transients are unique probes of the active sites of serine enzymes because they present the enzymes with an evolutionarily unanticipated task to accommodate a crowded trigonal bipyramidal structure. One of the important observations to report in this paper is that each ligand in phosphorus is engaged in binding with a key active-site component in the pentacoordinate P_SC_S diastereomer of soman-inhibited AChE. This mode of binding is reminiscent of the binding of acetylcholine, the natural substrate. Not all ligands can favorably interact in the resting structure with an active-site feature of the enzyme in the P_RC_S diastereomer; but, if skeletal motions are allowed, the pinacolyl group is accommodated at the acyl binding site as it might be the case in the reaction of butyrylcholine.

One of the distinguishing features of the crystal structure of *Torpedo californica* (*Tc)* AChE[1] is the *short H-bonds in the catalytic triad*. Notably, the His440 Nδ---OOCβ Asp327 bond distance is 2.5 Å (2.8 Å resolution) and 0.2 Å shorter than the corresponding H-bond in trypsin[23−25] and chymotrypsin (1.5 Å resolution). The distances between H-donors and acceptors at the active site of serine proteases ensuing His protonation or covalent modification was measured by NMR and reported to be shortened by 0.1−0.2 Å.[26] We reported similar observations using molecular mechanics calculations on the tetracoordinate adducts of soman-inhibited AChE, trypsin and chymotrypsin.[7] Remarkably, all the above are also consistent with results of proton inventory measurements on transition states of enzymic acyl transfer reactions.[27,28] Proton inventory measurements on the hydrolysis of acetylcholine or phenyl acetate catalyzed by AChE and those on the reactions of specific oligopeptides catalyzed by chymotrypsin and trypsin give different results: AChE reactions show only single-proton catalysis,[17,29,30] whereas the serine protease reactions in question show multiproton catalysis.[28] The latter were attributed by Schowen to tightening and strengthening of the H-bond network in the catalytic triad

(15) (a) Kovach, I. M.; Huber-Ashley Harmon, J.; Schowen, R. L. *J. Am. Chem. Soc.* **1988**, *110*, 590−593. (b) Kovach. I. M. unpublished data on the inactivation of serine proteases by soman.

(16) Bennet, A. J.; Kovach, I. M.; Bibbs, J. A. *J. Am. Chem. Soc.* **1989**, *111*, 6424−6427.

(17) Kovach, I. M.; Larson, M.; Schowen, R. L. *J. Am. Chem. Soc.* **1986**, *108*, 3054−3056.

(18) Bennet, A.; Kovach, I. M.; Schowen, R. L. *J. Am. Chem. Soc.* **1988**, *110*, 7892−7893.

(19) Boter, H. L.; Ooms, A. J. *Biochem. Pharmacol.* **1967**, *16*, 1563−1569.

(20) De Jong, L. P. A.; Benschop, H. P. In *Stereoselectivity of Pesticides*; Ariens, E. J., van Rensen, J. J. S., Welling, W., Eds.; Elsevier: Amsterdam, 1988; pp 109−149.

(21) Ooms, A. J. J.; van Dijk, C. *Biochem. Pharmacol.* **1966**, *15*, 1361−1377.

(22) Bencsura, A.; Enyedy, I.; Viragh, C.; Akhmetshin, R.; Kovach, I. M. In *Proceedings of the Fifth International Meeting on Cholinesterases, Madras, India* Quinn, M. D., Doctor, B. P., Eds.; Plenum Publishing. Co.: New York, 1995; pp 155−162.

(23) Chambers, J. L.; Stroud, R. M. *Acta Crystallogr., Sect. B* **1977**, *33*, 1824.

(24) Kossiakoff, A. A.; Spencer, S. A. *Biochemistry* **1981**, *20*, 6462−6474.

(25) James, M. N. G. *Can. J. Biochem.* **1980**, *58*, 251−272.

(26) Frey, P. A.; Whitt, S. A.; Tobin, J. B. *Science* **1994**, *264*, 1927−1930.

(27) Quinn, D. M.; Sutton, L. D. In *Enzyme Mechanism from Isotope Effects*; Cook, P. F., Ed.; CRC Press: Boston, MA, 1991; pp 73−126.

(28) Venkatasuban, K. S.; Schowen, R. L. *CRC Crit. Rev. Biochem.* **1985**, *17*, 1−44.

(29) Quinn, D. M. *Chem. Rev.* **1987**, *87*, 955−975.

(30) Quinn, D. M.; Pryor, A. N.; Selwood, T.; Lee, B. H.; Acheson, S. A.; Barlow, P. N. In *Cholinesterases: Structure, Function, Mechanism, Genetics, and Cell Biology*; Massoulie, J., Bacou, F., Barnard, E., Chatonnet, A., Doctor, B. P., Quinn, D. M., Eds.; American Chemical Society: Washington DC, 1991; pp 252−257.

Table 1. Distances below 5 Å and Angles (deg, in parentheses) in Key Interactions at the Active Site in the Diastereomers of Soman-Inhibited AChE[a,b]

			P_SC_S				P_RC_S			
interaction		native	TC		PC		TC		PC	
HisNϵ-H---OESer	3.1	3.12 ± 0.23	2.77 (143)	3.15 ± 0.20 (136 ± 27)	2.71 (166)	2.78 ± 0.10 (164 ± 9)	2.75 (148)	3.35 ± 0.19 (104 ± 10)	2.83 (144)	3.46 ± 0.28 (80 ± 8)
HisNδ-H---O2Glu	2.5	2.70 ± 0.01	2.61 (146)	2.59 ± 0.06 (164 ± 7)	2.55 (137)	2.62 ± 0.07 (166 ± 7)	2.63 (149)	2.60 ± 0.06 (168 ± 6)	2.65 (141)	2.60 ± 0.07 (165 ± 8)
HisNϵ-H---OEP			3.42 (150)	3.98 ± 0.30 (102 ± 16)		3.44 ± 0.22 (112 ± 7)	4.43 (149)	5.14 ± 0.16 (95 ± 9)		4.86 ± 0.27 (61 ± 8)
Gly118N-H---OPP			3.11 (165)	3.83 ± 0.26 (61 ± 10)	2.99 (161)	2.84 ± 0.12 (160 ± 10)				4.10 ± 0.26 (54 ± 10)
Gly119N-H---OPP			2.76 (157)	2.79 ± 0.12 (148 ± 0.12)	2.69 (161)	2.79 ± 0.11 (166 ± 9)	4.76 (121)	4.28 ± 0.31 (51 ± 9)		2.87 ± 0.14 (163 ± 9)
Ala201N-H---OPP			2.85 (115)	2.96 ± 0.13 (147 ± 12)	2.98 (120)	3.28 ± 0.17 (160 ± 10)		3.26 ± 0.24 (119 ± 14)		2.94 ± 0.15 (149 ± 13)
INHOEP---Gly118			4.07			4.88 ± 0.18				
HisNϵ-H---OPP							3.17 (137)		2.66 (142)	

[a] Parameters under each heading are from the crystal structure[1] for the native and from the YETI-optimized structure for the adducts in the first column and for the last 40 ps, with standard errors, of the simulations by CHARMM at 300 K in the second column. [b] TC tetracoordinate P, PC pentacoordinate P.

Table 2. Distances (Å) and Angles (deg, in parentheses) in Key Interactions at the Active Site in the Diastereomers of Soman-Inhibited Trypsin[a,b]

			P_SC_S				P_RC_S	
interaction		native	TC		PC		TC	PC
HisNϵ-H---OESer	3.0	4.10 ± 0.31	3.11 (131)	3.24 ± 0.25 (135 ± 16)	2.95 (137)	3.03 ± 0.24 (151 ± 15)	3.09 (115)	2.91 (131)
HisNδ-H---O2Asp	2.7	2.91 ± 0.16	2.66 (142)	2.83 ± 0.12 (123 ± 11)	2.60 (126)	2.79 ± 0.13 (131 ± 16)	2.81 (167)	2.63 (138)
HisNϵ-H---OEP			3.93 (166)	4.44 ± 0.29 (150 ± 11)	3.96 (165)	4.83 ± 0.26 (151±11)	2.98 (174)	3.08 (141)
Gly193N-H---OPP			2.71 (150)	2.73 ± 0.09 (164 ± 8)	2.78 (154)	2.84 ± 0.13 (152 ± 12)	2.81 (156)	2.78 (151)
Ser195N-H---OPP			2.86 (149)	3.05 ± 0.18 (151 ± 8)	2.75 (149)	3.38±0.29 (146 ± 8)	2.78 (147)	2.70 (149)

[a] Parameters under each heading are from the crystal structure[33] for the native and from the YETI-optimized structure for the adducts in the first column and for the last 40 ps, with standard errors, of 120 ps simulations by CHARMM at 300 K in the second column. [b] TC tetracoordinate P, PC pentacoordinate P.

at the transition state as a result of the compression exerted by the best-fitting substrates.[28] In contrast, AChE evolved to work on a small substrate that provides few leverages to exert the needed compression.[14] Yet hydrolysis of the natural substrate by AChE is more efficient than catalysis of peptide hydrolysis by most serine proteases.

Molecular dynamics (MD) simulations of the optimized structures of native AChE and its adducts, reported herein, give insight into how the skeletal motions accommodate an overcrowded active site particularly in the pentacoordinate adduct. An analysis of the MD simulation of the native AChE shows a tight catalytic triad already "wound" in the reactant state to act on the substrate. As skeletal motions are allowed, the H-bond distance between His440 and Glu327 increases by ~10%. Key H-bond distances at the active site are further shortened by 0.05−0.3 Å in energy-minimized structures of the adducts of AChE covalently modified by soman at the pentacoordinate and tetracoordinate intermediate stage. Any relief that may stem from the skeletal motion is balanced by a repositioning of Glu199 closer to the catalytic triad and phosphonyl fragment. This subtle reorientation of active-site residues should be relevant to the great catalytic efficiency of AChE and may indicate adaptability to alternate catalytic mechanisms.[7]

Results

Generation of the Parameters for Phosphonate Fragments. The geometric and charge parameters for the pentacoordinate phosphonate fragment were obtained from an *ab initio* calculation using a model compound generated in GAMESS[31] by a 6-31*G** basis set and requisite parameters in CHARMM[32] were generated accordingly. The tetracoordinate phosphonate fragment was built and energy-optimized using MNDO/MOPAC described earlier.[7,33]

Molecular Mechanics. Fully solvated and energy-optimized proteins were obtained using the X-ray coordinates of AChE,[1] trypsin[34] and chymotrypsin,[35] also published earlier.[7,33] In the structure (II) for the P_RC_S diastereomer of AChE, the phosphoryl group was accommodated near the $HisH^+440$, and the methyl group was placed near the oxyanion hole while the pinacolyl group occupied the vicinity of Trp84, the only reasonable binding site for this bulky group in the crystal structure. The geometric parameters for nonbonded interactions in the pentacoordinate and tetracoordinate P_SC_S and P_RC_S adducts of soman-inhibited AChE, trypsin and chymotrypsin were calculated in molecular mechanics program YETI (5.3),[36] and the critical interactions are in the first column of Tables 1−3. Protein−

(31) Schmidt, M. W.; Baldridge, K. K.; Boatz, J. A.; Elbert, S. T.; Gordon, M. S.; Jensen, J. J.; Kosecki, S.; Matsunaga, N.; Nguyen, K. A.; Su, S.; Windus, T. L.; Dupuis, M.; Montgomery, J. A. *J. Comput. Chem.* **1993**, *14*, 1347−1363.
(32) Brooks, B. R.; Bruccoleri, R. E.; Olafson, B. D.; States, D. J.; Swaminathan, S.; Karplus, M. *J. Comput. Chem.* **1983**, *4*, 187−217.
(33) Zhao, Q.; Kovach, I. M.; Bencsura, A.; Papathanassiu, A. *Biochemistry* **1994**, *33*, 8128−8138.
(34) Walter, J.; Steigemann, W.; Singh, T. P.; Bartunik, H.; Bode, W.; Huber, R. *Acta Crystallogr., Sect. B* **1982**, *38*, 1462−1472.
(35) Dixon, M. M.; Mathews, B. W. *Biochemistry* **1989**, *28*, 7033−7038.

Table 3. Distances (Å) and Angles (deg, in parentheses) in Key Interactions at the Active Site in the YETI-Optimized Structure of the Diastereomers of Soman-Inhibited Chymotrypsin[b]

		P_SC_S		P_RC_S	
interaction	native[a]	TC	PC	TC	PC
HisNϵ-H---OESer	3.2	2.92	2.78	2.90	2.63
		(134)	(149)	(117)	(132)
HisNδ-H---O2Asp	2.7	2.68	2.57	2.83	2.70
		(145)	(134)	(169)	(146)
HisNϵ-H---OEP		3.67	4.52	2.92	3.12
		(152)	(164)	(168)	(149)
Gly193N-H---OPP		2.69	2.76	2.81	2.80
		(140)	(145)	(146)	(152)
Ser195N-H---OPP		2.79	2.85	2.75	2.87
		(153)	(139)	(148)	(145)

[a] Crystal structure.[34] [b] TC tetracoordinate P, PC pentacoordinate P.

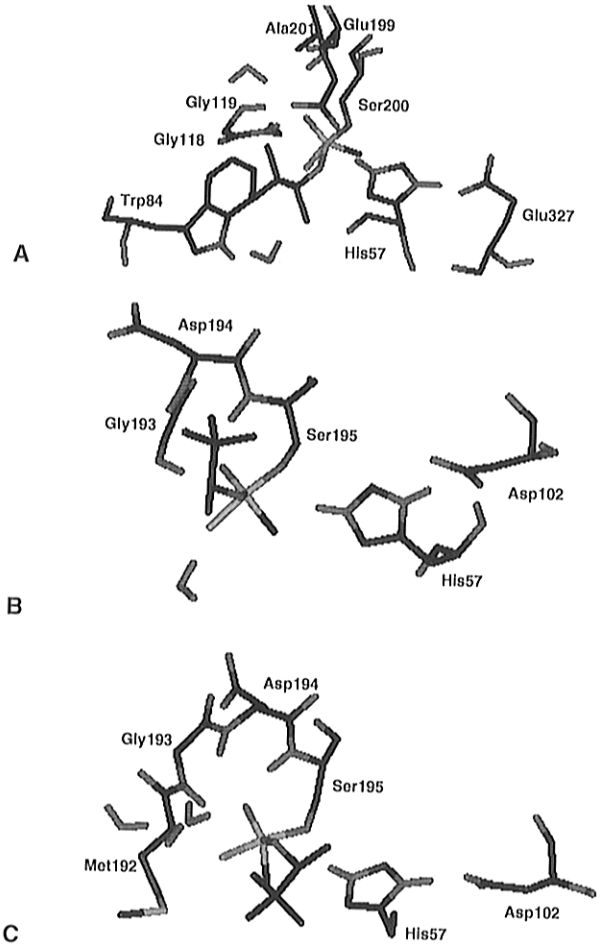

Figure 1. Active-site interactions in the energy-minimized (YETI) pentacoordinate P_SC_S diastereomers of soman-inhibited: A, AChE; B, trypsin; and C, chymotrypsin.

protein interaction energies were within 5 kcal/mol for each adduct of an enzyme and protein−water interactions were within 100 kcal/mol corresponding to no more than a difference of 2−8 water molecules. A notable feature of the data in the first column of the tables is the shortening of the distance between Ser and $HisH^+$ and expansion of the distance between $HisH^+$ and Glu/Asp in the catalytic triad in the covalently modified enzymes. Figures 1 and 2 show the geometry-optimized active sites of the diastereomers of the pentacoordinate adducts of soman-inhibited AChE, trypsin and chymotrypsin.

(36) (a) Vedani, A.; Huhta, D. V.; Jacober, S. P. *J. Am. Chem. Soc.* **1989**, *111*, 4075−4080. (b) Vedani, A. J. *J. Comput. Chem.* **1988**, *9*, 269−280.

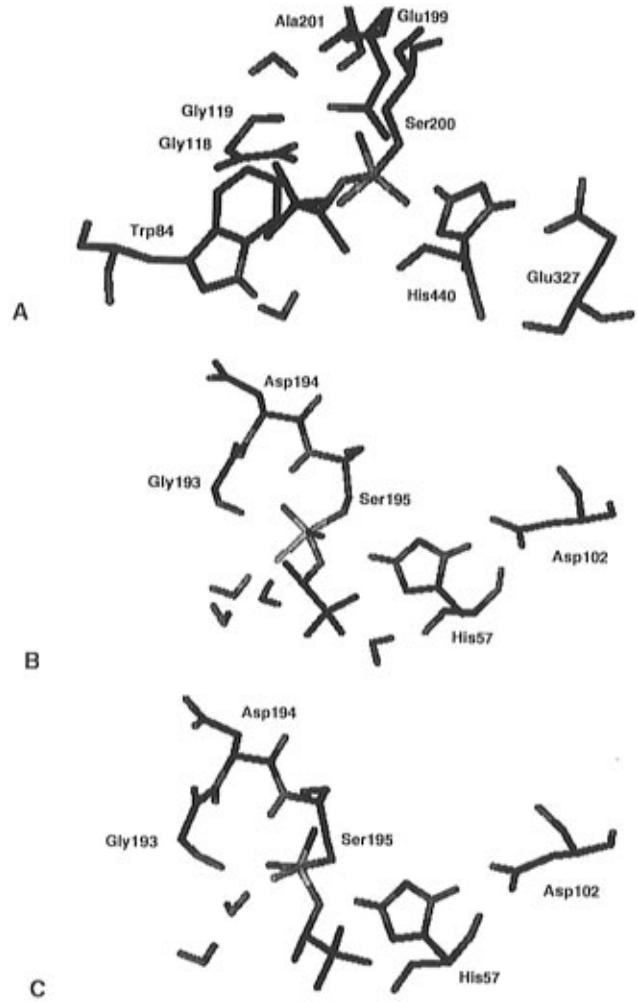

Figure 2. Active-site interactions in the energy-minimized (YETI) pentacoordinate P_RC_S dieastereomers of soman-inhibited: A, AChE; B, trypsin; and C, chymotrypsin.

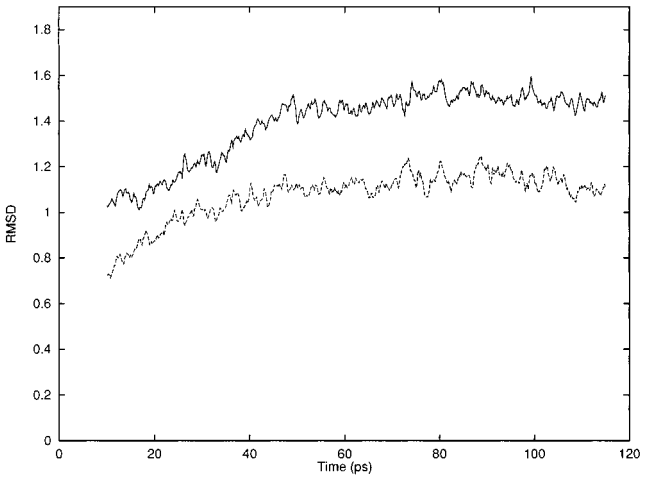

Figure 3. Time dependence of the rmsd for 100 ps of a 120 ps full simulation of (—) AChE and (- -) trypsin.

Molecular Dynamics Using CHARMM.[32] Fully solvated native *Tc*AChE and trypsin were studied in 120 ps simulations with particular attention to the mobility of the active-site components. Figure 3 illustrates the root mean square deviation (rmsd) of all residues in AChE and trypsin in time dependence. Identical simulations were performed at 300 K with pentacoordinate and tetracoordinate P_SC_S adducts of soman-inhibited trypsin for the sake of comparing the mobility of the active-

Table 4. Mass Weighted Root Mean Square Deviation (rmsd, Å) from the X-ray Structure of AChE for the Average Structures Obtained in the Last 50 ps of Each Simulation and the Mass Weighted Isotropic Fluctuation (Δr^2, Å^2) around the Average Structures[a,b]

		P_SC_S		P_RC_S	
atoms	native	PC	TC	PC	TC
		rmsd			
protein residues	1.63	1.42	1.37	1.57	1.70
backbone	1.24	1.00	0.97	1.07	1.09
Phe288	0.14	0.88	1.24	2.13	2.80
Phe290	0.32	0.65	0.95	0.77	1.09
Trp233	0.19	0.80	0.95	0.96	1.12
		Δr^2			
protein residues	0.45	0.18	0.12	0.11	0.12
backbone	0.23	0.10	0.06	0.05	0.06
Phe288	0.23	0.12	0.12	0.13	0.17
Phe290	0.45	0.13	0.13	0.16	0.16
Trp233	0.22	0.15	0.17	0.14	0.21

[a] All values were calculated for core residues in a sphere of 18 Å radius around Ser200 constituting the reaction zone in the stochastic boundary calculations for the adducts. Although the native enzyme was subjected to a full simulation, the data for it was generated consistently with the rest. [b] TC tetracoordinate P, PC pentacoordinate P.

site components. To reduce the computational demands, the pentacoordinate and tetracoordinate diasteromeric adducts of soman-inhibited AChE were studied with stochastic boundary dynamics calculations at 300 K. Additionally, the equilibrium structures of tetracoordinate and pentacoordinate phosphonate esters of both diastereomers of the soman-inhibited AChE were heated to 700 K and cooled down slowly.

Simulations were carried out for two starting conformations of the P_RC_S diastereomer: In one case, structure I, the phosphoryl group was placed into the oxyanion hole and the pinacolyl group was forced against the acyl binding region. Structure II, optimized in YETI, was the other starting structure. In the course of dynamics, amino acid residues Phe290, Phe288, and Trp233 moved to accommodate the pinacolyl side chain in structure I. In this relaxed form, structure I had fewer unfavorable interactions than structure II. Structure II had also changed greatly after the first 20 ps simulation at 300 K: It rotated into a conformation in which the phosphoryl fragment and the oxyanion hole moved closer together, while a substantial rotation around the Cα−Cβ bond moved the *tert*-butyl group of the pinacolyl side chain into binding distance with Trp84. Trp84 in response moved lower, while Trp233 moved up to interact with one of the methyl groups of the *tert*-butyl fragment. The energy of interaction between inhibitor and protein became nearly the same as that in structure I but with a larger standard error. The second columns given in Table 1 for each structure, I for the P_RC_S adducts, provide critical distances at the active site obtained as average for the last 40 ps of the simulation. Note that the geometries for these interactions are more favorable for the P_SC_S than for the P_RC_S diastereomers. The tetracoordinate P_SC_S diastereomer of soman-inhibited AChE was further perturbed by heating to 1500 K and then cooling it slowly; but no major rearrangement resulted from this stress on the system. Only the pinacolyl side chain of this structure went under significant torsional change during the simulation, other features remained unchanged. Table 2 lists critical distances for the last 40 ps of the 120 ps simulations in the native and P_SC_S adducts of soman-inhibited trypsin.

The rmsd in the equilibrium structures, averaged for the last 50 ps simulation at 300 K, from the X-ray crystallographic coordinates were within 1.1−1.7 Å for the average of all protein residues and 0.8−1.24 Å for the backbone: Tables 4 and 5

Table 5. Mass Weighted Root Mean Square Deviation (rmsd, Å) from the X-ray Structure of Trypsin for the Average Structures Obtained in the Last 50 ps of Full-Scale MD Simulations and the Mass Weighted Isotropic Fluctuation (Δr^2, Å^2) around the Average Structures[a]

			P_SC_S			
	native		PC		TC	
atoms	rmsd	Δr^2	rmsd	Δr^2	rmsd	Δr^2
protein residues	1.18	0.35	1.09	0.37	1.20	0.33
backbone	0.85	0.21	0.84	0.22	0.90	0.20

[a] TC tetracoordinate P, PC pentacoordinate P.

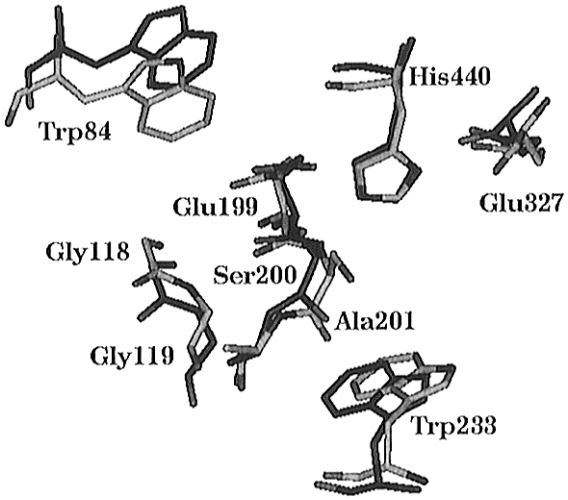

Figure 4. Comparison of the position of active-site residues for the average of the last 50 ps of a 120 ps full dynamics simulation (grey) with the X-ray structure (black) of AChE: the backbones of Ser200 were aligned.

contain the average rmsd and fluctuation of all protein residues, backbone and selected residues. The equilibrium structures were then analyzed for the binding mode of the phosphonate fragment in each conformation and for differences in stability of the tetracoordinate and corresponding pentacoordinate diastereomeric adducts. Figure 4 demonstrates the average conformation of active-site residues in the last 50 ps of a 120 ps dynamics simulation of native *Tc*AChE compared to the X-ray structure. Figures 5 and 6 show the average of structures during the last 50 ps of 200 ps stochastic boundary dynamics of the active-site residues in the pentacoordinate soman-inhibited AChE structures compared to the crystal structure. Figure 6 also gives a pictorial representation of the movement of $HisH^+440$ in the course of MD simulation of the pentacoordinate P_RC_S diastereomer (I) of soman-inhibited AChE. Figure 7 illustrates the last 100 ps MD simulation of the pentacoordinate P_SC_S diastereomer of soman-inhibited AChE in 10 snapshots at 10 ps intervals. Figures 8−10 compare time-series of distances between key atoms of active-site residues and the phosphonate fragment in native AChE and its covalently modified forms. Figures 11 and 12 show time series for distances within the catalytic triad for native trypsin and its pentacoordinate and tetracoordinate P_SC_S adducts with soman. Table 6 provides the energy partitioning for the inhibitor fragment in each adduct. The protein−protein, protein−water, water−water interaction energies were consistent, but to a lesser extent, due to the minor inequities in the number of solvent molecules within the reaction zone for the stochastic boundary calculations. Continuation of this project will include full simulations and free energy calculations for the AChE adducts.

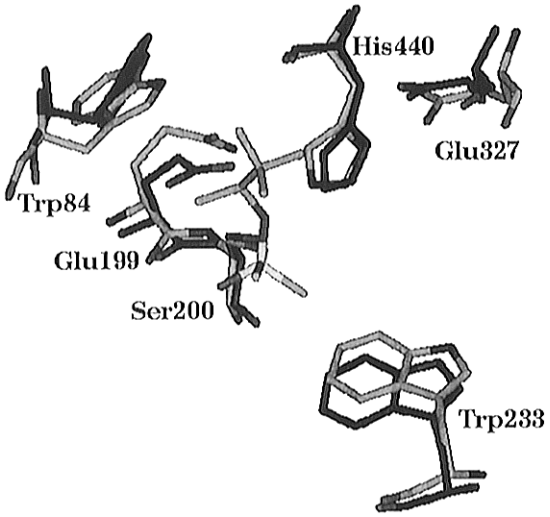

Figure 5. Comparison of the active-site residues of the average structure for the last 50 ps of a 200 ps stochastic boundary simulation of the pentacoordinate P_SC_S diastereomer of soman-inhibited AChE (grey) with the X-ray structure of AChE (black): the backbones of Ser200 were aligned.

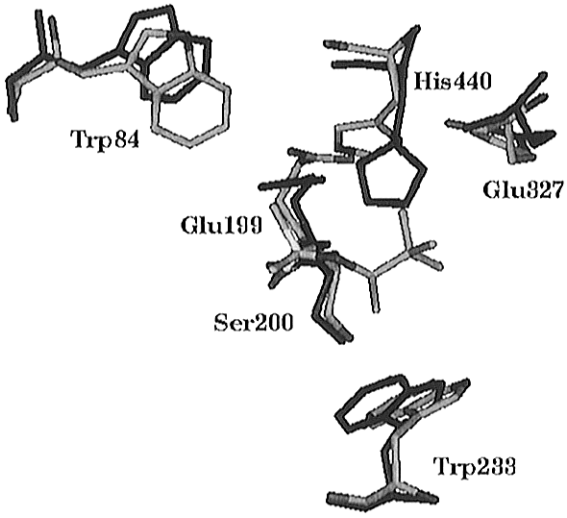

Figure 6. Comparison of the active-site residues of the average structure for the last 50 ps of a 200 ps stochastic boundary simulation of the pentacoordinate P_RC_S diastereomer of soman-inhibited AChE (grey) with the X-ray structure of AChE (black): the backbones of Ser200 were aligned.

Discussion

Comparison of the Initial Equilibrium Structures of the Covalently-Modified Active Site of the Three Enzymes. All three serine hydrolase enzymes of this study showed stereoselectivity for the levorotatory isomers of soman, which have been assigned P_S configuration based on chemical correlations:[19,20] the selectivity of $>10^4$ for AChE[19] translates into $\Delta\Delta G^{\ddagger} > 5.6$ kcal/mol difference in transition state free energies. AChE also showed stereoselectivity for the *S* configuration at P in a series of chiral thiocholinphosphonate esters.[37]

If the stereochemical outcome of phosphonylation of the active-site Ser is inversion of configuration, as implied by eq 1, then the P_SC_S diastereomer would be the product of phosphonylation by the P_SC_S diastereomer of soman. Both configurations around P were considered in the evaluation of the critical interactions between protein and inhibitor fragment. Based on experimental data on phosphorylated serine hydrolases, the oxyanion hole interaction with phosphoryl was considered to be critical.[38,39] It could be readily satisfied, while restricting molecular motions to the side chains only in program YETI, in building the P_SC_S diastereomers but not in the P_RC_S diastereomers of soman-inhibited AChE. There was only one way to accommodate either the pentacoordinate or tetracoordinate P_RC_S diastereomer of soman-inhibited AChE into the native conformation of the enzyme, that is with the methyl group in the oxyanion binding area and the pinacolyl group binding against Trp84.

The energy-optimized structures of pentacoordinate and tetracoordinate[7] soman-inhibited AChE show that electrostatic and hydrophobic forces in the active-site gorge lock the phosphonate fragment and allow a minimal motion of the amino acid side chains. A striking feature of the results is the very crowded and dry active site of AChE in all adducts (Table 1 and Figures 1 and 2). There are three experimental water molecules at the active site after covalent modification and neither of the two methods of protein solvation (YETI and CHARMM) resulted in a higher population of water molecules at the active site because of its very hydrophobic character. Two of the crystallographic water molecules seem to have significant stabilizing role: One solvates Glu443, independently of its protonation state, and the other interlocks Glu199 and Tyr130. The two Glu residues occupy a plane above the catalytic triad but do not seem to be connected by a solvating water molecule as suggested earlier.[40] This was tested in our calculations with and without protonation of Glu443. The H-bonding network to Tyr130 is responsible for the unique position of Glu199, above the plane formed by the catalytic triad.

As earlier, we take note of the conformation that enables *Glu199 to exert a strong electrostatic catalytic effect* on most reactions.[7] A multifunctional role of Glu199 in AChE was suggested earlier.[6,7] Subsequently, the Glu199Gln mutation in AChE was made and found to cause a significant rate reduction in the reactions of substrates and inhibitors.[2,40,41] This catalytic effect of Glu199 stands in stark contrast to the role of the corresponding Asp residues conserved in serine proteases. Asp194 preceding the catalytic Ser, fulfills a critical role in activation of the zymogen into the mature enzyme: A result of this activation is the formation of the oxyanion hole by a major conformational rearrangement of the acid side chain of Asp194 to engage in a salt bridge with Ilu16.[39] We contend that the oxyanion hole in AChE, and other hydrolases,[4] evolved quite differently and without the participation of the catalytic Ser residue as H-donor.

The active sites of native trypsin and chymotrypsin are more solvated in both the native and the covalently modified formes than in AChE. Even the pentacoordinate phosphonylated equilibrium structures are not particularly crowded as shown in Tables 2 and 3.

Molecular Dynamics Simulation of the Native Enzymes. Mobility of the constituents of the active site in the solution structure of the adducts and compared under identical conditions to the native enzyme was one focus of this study. Limited mobility of the catalytic triad and a sensitivity of local

(37) Hosea, N. A.; Berman, H. A.; Taylor, P. *Biochemistry* **1995**, *34*, 11528−11536.

(38) Stroud, R. M.; Kay, L.; Dickerson, R. E. *J. Mol. Biol.* **1974**, *83*, 185−208.

(39) (a) Polgar, L. *Mechanisms of Protease Action*; CRC Press, Inc.: Boca Raton, FL, 1990. (b) Polgar, L. In *Hydrolytic Enzymes*; Neuberger, A., Brocklehurst, K., Eds.; Elsevier Sci. Pub. Co.: Amsterdam, 1987; pp 159−200.

(40) Ordentlich, A.; Kronman, C.; Barak, D.; Stein, D.; Ariel, N.; Marcus, D.; Velan, B.; Shafferman, A. *FEBS Lett.* **1993**, *334*, 215−220.

(41) Saxena, A.; Doctor, B. P.; Maxwell, D. M.; Lenz, D. E.; Radic, Z.; Taylor, P. *Biochem. Biophys. Res. Commun.* **1993**, *197*, 343−349.

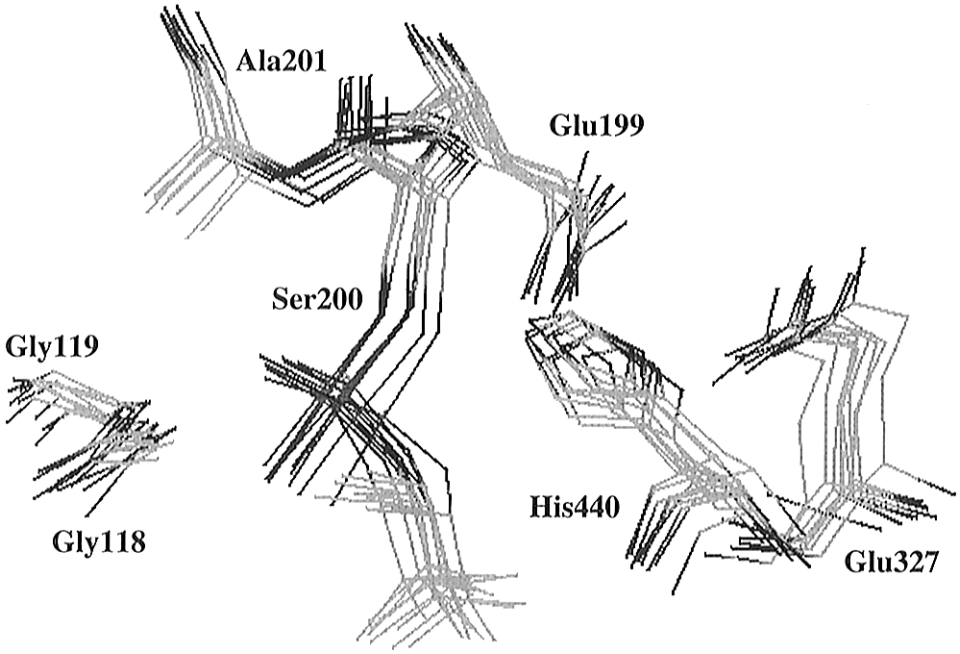

Figure 7. The last 100 ps excerpt of a 200 ps stochastic boundary simulation of the pentacoordinate P_SC_S diastereomer of soman-inhibited AChE: snapshots at 10 ps.

Table 6. Differences in the Sum of Protein−Fragment (P−F), Water−Fragment (W−F), and Fragment−Fragment (F−F) Interaction Energies (kcal/mol), among Phosphonate Adducts of AChE and Trypsin as Calculated in CHARMM[a]

adduct[a]	P−F	W−F	F−F	total
AChE-P_SC_S PC	−106.7	−7.2	−41.6	−155.5
AChE-P_SC_S TC	−67.9	−0.5	−60.2	−128.0
AChE-P_RC_S PC	−109.9	2.9	−43.8	−150.7
AChE-P_RC_S TC	−59.8	−1.0	−62.5	−123.3
trypsin-P_SC_S PC	−74.2	−63.3	−74.2	−211.7
trypsin-P_SC_S TC	−53.6	−14.5	−53.7	−121.8

[a] TC tetracoordinate P, PC pentacoordinate P.

conformations to the presence of small cations binding to Trp84 were observed during a MD refinement of the X-ray structure of the *Tc*AChE dimer.[12] In our full MD simulation of the solution structure of the AChE monomer, the rmsd of protein residues within the 18 Å radius from Ser200 Oγ from the X-ray structure was 1.63 Å in the last 50 ps. The corresponding rmsd for the backbone was 1.24 Å. The catalytic residues of the triad stayed within 0.3 Å of the X-ray-defined position, while the greatest mobility was observed for residues 199, 290, and others near the surface (Table 4). The variance reflects on significant fluctuations around the average structure. Table 1 and Figures 8 and 9 illustrate that the distance between the Ser200 Oγ and His440 Nϵ in AChE remained very close to the value in the X-ray structure in the last 50 ps of a 120 ps simulation, but the His440 Nδ-Glu327 COO^- distance increased by nearly 0.2 Å with respect to the X-ray structure. Moreover, the His440 Nϵ-Glu199 COO^- distance was around 4.3 Å versus 3.8 Å in the X-ray structure, although occasional closer contacts were observed when His440 moved away from Ser200. The propensity of Glu199 for interacting with Ser200 or a water molecule has been examined in our earlier work, because this residue was implicated as a surrogate general base catalyst in the reaction of bulky substrates.[7] The possibility for interaction between Ser200 and Glu199 may be remote in the native structure but enhanced when the active site of AChE is modified with large effectors.

Glu199 is solvated by a conserved water molecule that also H-bonds to either the carbonyl oxygen or the amide N in

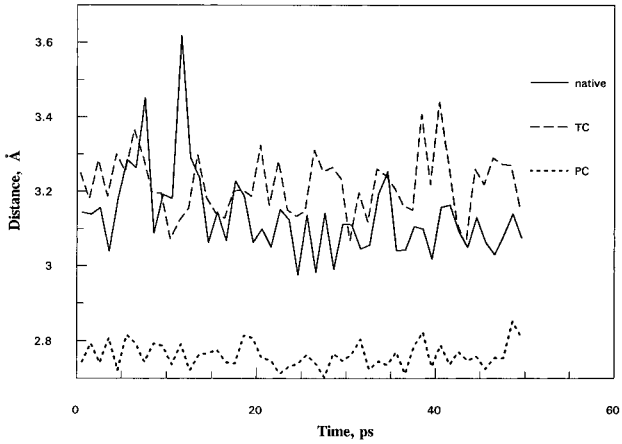

Figure 8. Time dependence of the Ser200 Oγ-His440 Nϵ distance in the last 50 ps of (a) a 120 ps simulation of native AChE and (b) a 200 ps stochastic boundary simulation of the pentacoordinate and tetracoordinate P_SC_S diastereomers of soman-inhibited AChE. Each point represents an average calculated for 2 ps.

Gly117. Gly117 is at the beginning of a loop part of which constitutes the oxyanion hole of AChE. Another important observation was the interaction of NH in Gly118, a constituent of the oxyanion hole, with Ser122 through a solvating water molecule conserved in the native structure as well. There is the opportunity for this water to bridge Ser122 to either Gly118 or to Tyr148 but probably not to both. Fluctuations of this loop can play a role in regulation of the size of the oxyanion hole in AChE.

The other loop of great importance is the omega loop[11] which moves correlated to the skeletal and torsional motion of Trp84 (Figure 4). The functional role of Trp84 and the omega loop is best seen when the active site is modified with an effector (*vide infra*).

Both the rmsd and fluctuation around the average structure were smaller in trypsin than in AChE (Figure 3, Table 5). The distances within the catalytic triad were greater in trypsin than in AChE as apparent in Tables 1 and 2 and in Figures 11 and 12. There is only a 15 ps residence time of Ser195 at 2.8 Å to

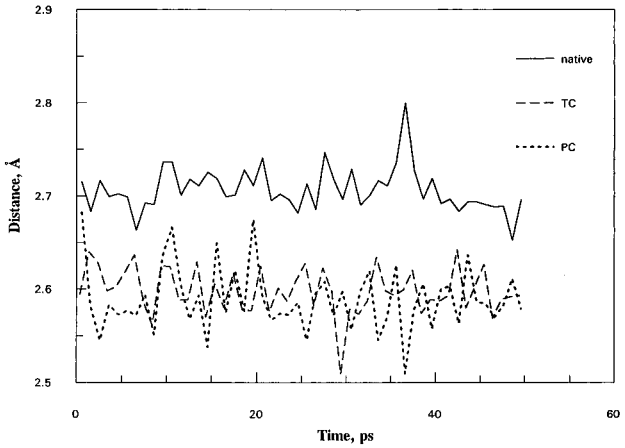

Figure 9. Time dependence of the Glu327 COO^--His440 Nδ distance in the last 50 ps of (a) 120 ps simulation of native AChE and (b) a 200 ps stochastic boundary simulation of the pentacoordinate and tetracoordinate P_SC_S diastereomers of soman-inhibited AChE. Each point represents an average calculated for 2 ps.

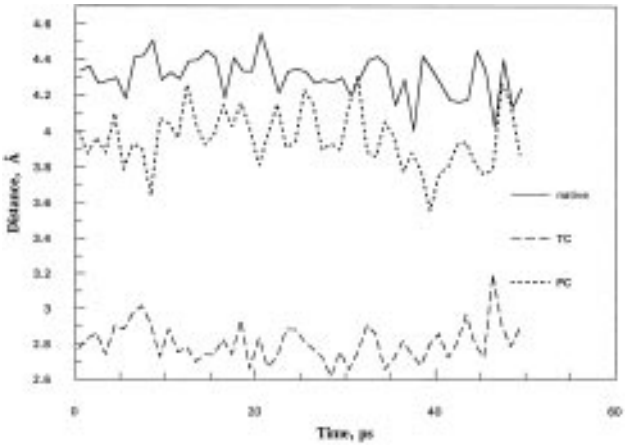

Figure 10. Time dependence of the Glu199 COO^--His440 Nδ distance in the last 50 ps of (a) a 120 ps simulation of native AChE and (b) a 200 ps stochastic boundary simulation of the pentacoordinate and tetracoordinate P_SC_S diastereomers of soman-inhibited AChE. Each point represents an average calculated for 2 ps.

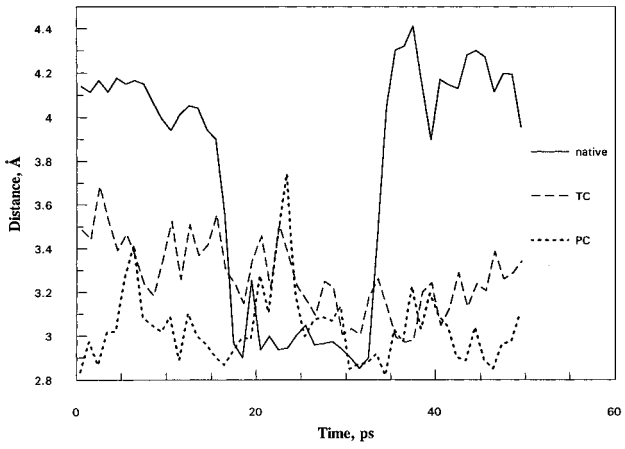

Figure 11. Time dependence of the Ser195 Oγ-His57 Nϵ distance in (a) native trypsin and (b) in its soman-inhibited P_SC_S adducts; last 50 ps of 120 ps simulations. Each point represents an average calculated for 2 ps.

H-bond with His57, while it is rotated away at 4.2 Å from His57 for the rest of the time in the last 50 ps time segment of the 120 ps simulation. The distance between His57 and Asp102 hovered around 2.9 Å in native trypsin.

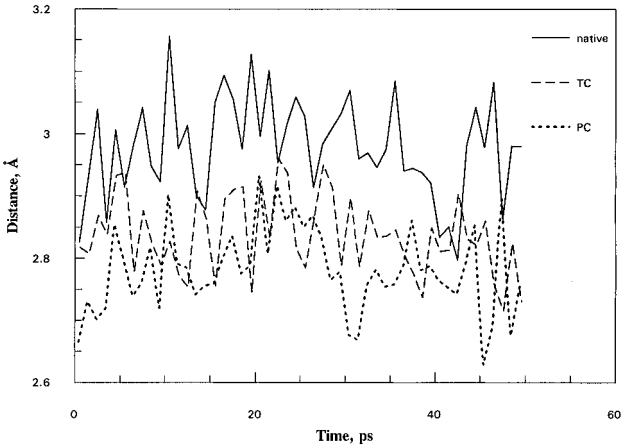

Figure 12. Time dependence of the Asp102 COO^--His57 Nδ distance in (a) native trypsin and (b) in its soman-inhibited P_SC_S adducts; last 50 ps of 120 simulations. Each point represents an average calculated for 2 ps.

Molecular Dynamics Simulation of the Pentacoordinate Soman-Inhibited Adducts of AChE. Stereoselectivity. The simulations involving the first transients formed immediately after covalent bond formation between the Ser200 Oγ and P of soman were critical in shedding light on the structural basis for stereoselectivity of AChE inactivation by soman: $\Delta\Delta G^{\ddagger} > 5.6$ kcal/mol, favoring the P_S diastereomers. This must stem from the great spacial restrictions observable on the equilibrium structures in Table 1 and Figures 1 and 2 when skeletal motion is prevented.

In both diastereomers of the pentacoordinate adducts of soman-inhibited AChE, the O^- ligand was placed in the equatorial plane according to the Westheimer guide lines.[42] The MD simulation maintained the overlap between phosphoryl and all three H-bond donors in the pentacoordinate and succeeding tetracoordinate structure of the P_SC_S diastereomer. Only a minor movement of the phosphonyl fragment occurred in the P_SC_S diastereomer except for the pinacolyl moiety: It moved significantly toward the Trp84 to provide an overlap that was greater than in the tetracoordinate structure. This interaction in the pentacoordinate transient *exerts a compression from the equatorial plane* of the trigonal bipyramid that could be *critical to the efficient elimination of the F^- leaving group* in the phosphonylation step by soman.

P_SC_S-Diastereomer. The equatorial ligands crowded $HisH^+$-440 and caused a compression of the $HisH^+$440 Nδ-Glu327 COO^- distance from 2.7 Å to 2.55 Å in the equilibrium structure of the pentacoordinate P_SC_S diastereomer (Table 1). Favorable electrostatic and H-bonding interactions in this structure are somewhat counterbalanced by van der Waals repulsions within the phosphonate fragment. Even when the backbone was allowed to relax, during the MD simulation, the crowding was not entirely relieved in this structure, and an interaction between $HisH^+$440 and Glu199 became significant. The strong electrostatic attraction between the two groups results, to some extent, from the limitation of the computational techniques we used. It is tempting to think that, in reality, the electrostatic interaction of Glu199 is with the phosphonyl fragment. It can reduce electron density by affecting P−F bond cleavage. The electrostatic "push" from Glu199 together with steric strain caused by binding the pinacolyl to Trp84 may be the very source of the prominent efficiency of leaving group departure in phosphonylation of AChE by the P_S diastereomers of soman.

(42) Westheimer, F. H. *Acc. Chem. Res.* **1968**, *1*, 70−78.

P_RC_S-Diastereomer. MD simulations gave the opportunity to remove the original constraint with the equilibrium structure (II) of the P_R diastereomer of soman-inhibited AChE. In spite of the possibility that the O^- gets close to $HisH^+440$ relieving the compression on the catalytic groups in structure II, this structure gives bad interactions between the methyl group and constituents of the oxyanion hole. Indeed, during the dynamics simulation at 300 K, the conformational barrier to accommodating the phosphoryl in the oxyanion hole was crossed, but the stabilizing interactions with Gly118, Gly119, and Ala201 remained inferior to those for the P_S diastereomer (Table 1). Gly118 alternated between H-bonding with the oxyanion for periods of 10 ps and interacting with Ser122 for periods of ~10 ps. This motion of Gly118 occurred with fluctuations of the loop 118−122 confirming the participation of this loop in the dynamics of AChE catalysis.

The pinacolyl group was moved concurrently into a favorable binding interaction with Trp84 initially. However, structure II in the new conformation was associated with a large fluctuation and a large error for inhibitor-protein interactions indicating that this mode of binding may be unproductive for phosphonylation of Ser200 in AChE. The Trp84-bound pinacolyl group then moved gradually toward Trp233 until the pinacolyl became sandwiched between the indole side chains similar to structure I (Figure 6) but with smaller displacements of Phe288 and Phe290. The average of the torsional angles in Trp84 for the last 40 ps after ~100 ps equilibration reflect the events: χ^1 is remarkably constant at −50−−60° in all structures except for the P_RC_S diastereomeric adduct; it is −71° in structure I and −82° in structure II. χ^2 changes from an average of 107° in the native structure and 122−127° in the P_SC_S adducts of soman-inhibited AChE to 51° and 82° for structure I and II, respectively, in the P_RC_S adducts.

Thus, structure I, with the phosphoryl oxygen facing the oxyanion hole, the methyl group near Trp84, and the pinacolyl group crowding the acyl binding site in the pentacoordinate structure, proved to be a realistic choice for a starting structure for MD. Table 4 shows the rmsd of residues in the acyl binding site to be the largest in the P_R adduct of soman-inhibited AChE. Residues Phe290 and Phe288 demonstrated significant mobility and other neighboring residues moved slightly in the region, but it was not enough. The binding of the pinacolyl moiety required a significant skeletal motion at Trp233 with some torsional adjustment. The rotational barrier was calculated to be ~30 kcal/mol for Trp233 at the acyl binding site of AChE. In comparison, the rotational barrier calculated for the indole side chain of free Trp is 45 kcal/mol.[43,44] $HisH^+440$ and Glu199 were also displaced from their original position by a steric interference with one of the methyl groups.

A third possible conformation, in which the pinacolyl moiety was placed in the oxyanion hole and the phosphoryl group faced $HisH^+440$, has also been explored. This conformation generated the least favorable interactions.

A salient conclusion of these simulations is that *the binding of the pinacolyl group is more favorable at Trp84 in the pentacoordinate P_SC_S diastereomer of the soman-inhibited AChE than that in any conformation of the P_RC_S diastereomer*. Figure 13 illustrates the difference in rmsd between the equilibrium structures of the diastereomers of the covalently modified AChE relative to the X-ray structure. More deviation in the P_R diastereomer than in the P_S diastereomer is clearly discernible, and the greatest skeletal displacement is at residues 440 and 233, 288 and 290 at the acyl binding site. Although the sum of the protein−inhibitor, inhibitor−inhibitor, inhibitor−water interactions are nearly the same in all structures (Table 6), there is a greater price to be paid for these in protein−protein interactions in the P_RC_S diastereomer than in the P_SC_S diastereomer. The energy for moving the side chains of residues at the acyl binding site must be invested into the accommodation of the transition state of the P_RC_S diastereomer of soman-inhibited AChE. It is tempting to point out the similarity of the ~5 kcal/mol difference in the sum of the energy terms between the pentacoordinate diastereomers to the $\Delta\Delta G^{\ddagger} > 5.6$ kcal/mol given by the kinetic data, but considering the nature of the energy calculations this may be fortuitous. Incidently, AChE-catalyzed hydrolysis of acetylcholine is favored by $\Delta\Delta G^{\ddagger} = 5$ kcal/mol (calculated from the kinetic data in ref 2) over that of butyrylcholine. Since the choline moiety of these substrates occupies the Trp84 binding site, the 5 kcal/mol difference must arise from the ease or difficulty of binding the acyl fragment.

The Pentacoordinate P_SC_S Adduct of Soman-Inhibited Trypsin. Distances within the catalytic triad of the pentacoordinate adduct became shorter than in the corresponding tetracoordinate adduct (Table 2). The leaving group in the phosphonyl fragment was far from $HisH^+57$ in the the trigonal bipyramid. This phenomenon is consistent with our earlier suggestion that the protonated His cannot donate its proton to the leaving group in the pentacoordinate structure, and thus it is not a good catalyst of leaving group departure from phosphonate esters.[7,14,45]

Molecular Dynamics Simulation of the Tetracoordinate Adducts of AChE and Trypsin with Soman. The P_SC_S diastereomer of soman-inhibited AChE was estimated to be 17−26 kcal/mol more stable than the P_RC_S diastereomer in our previous work.[7] The discriminating interaction was anticipated to be the three H-bonds with the phosphoryl group in the oxyanion hole. This requirement could not be easily met for the P_RC_S diastereomer, because it would have forced the bulky pinacolyl group to clash with residues of the acyl binding site,[7] *vide supra*. The energy-optimized structure (II) for the P_RC_S diastereomer of the soman-inhibited AChE had the methyl group partly in the oxyanion hole and the O^- was against the protonated $HisH^+440$, while the pinacolyl group occupied the same general area as in the P_SC_S diastereomer.

The earlier conformations of both diastereomers were now challenged: The P_SC_S diastereomer was heated to 700 K and then to 1500 K and allowed to find the minimum-energy conformation. Heating to 1500 K caused rapid rotational and torsional motions in amino acid side chains and in the alkyl side chain of the phosphonyl fragment, but did not cause disruption of the conformational integrity of the protein. In case of the P_RC_S diastereomer, two starting conformations were generated as described above. The structures were heated to 700 K and then cooled slowly to 300 K. While the torsional motions accelerated, the energy barrier separating the two conformations was not crossed. In structure II, the backbone adjusted to a conformation in which the oxyanion was pushed close to $HisH^+440$ and the two were held together by electrostatic forces. The transition observed with the pentacoordinate structure did not occur during a 200 ps simulation. A likely reason for it is that in the course of a putative rotation, the pinacolyl group would lose contact with any reasonable binding site in the tetracoordinate form of structure II.

Again, the only viable structure was structure I with the phosphoryl group in the oxyanion hole and the pinacolyl group bound in the acyl binding region. Structure I had the lowest

(43) McCammon, J. A.; Harvey, S. C. *Dynamics of Proteins and Nucleic Acids*; Cambridge University Press: Cambridge, 1989; pp 1−234.
(44) Karplus, M.; McCammon, J. A. *CRC Crit. Rev. Biochem.* **1981**, 293−349.

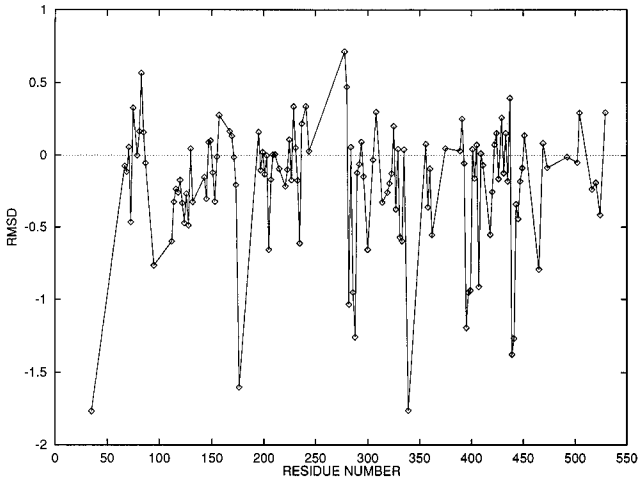

Figure 13. Differences in the rmsd relative to the X-ray structure of native *Tc*AChE between the pentacoordinate P_SC_S and P_RC_S diastereomores of soman-inhibited AChE {rmsd(P_SC_S) − rmsd(P_RC_S)} for all residues.

energy after the heating/cooling cycle and 120 ps simulation, although the oxyanion interactions were even weaker than in the pentacoordinate precursor (Table 1). Nevertheless, the binding of the pinacolyl group in structure I of the tetracoordinate P_RC_S soman-inhibited AChE seems to be a good model for the tetrahedral intermediate in the reaction of AChE with cholinesters having larger acyl fragments.

The equilibrium structures for the tetracoordinate diastereomers of the soman-inhibited trypsin and chymotrypsin were characterized in detail earlier.[7] The distinction between the diastereomers was much smaller than in AChE, and the active site was less crowded. MD simulation of the tetracoordinate P_SC_S adduct of the soman-inhibited trypsin showed that $HisH^+$-57 remained stable at 3.4 Å from the phosphonylated Ser195 (Figure 11) unlike in the native enzyme.

Mobility of Key Active-Site Components and the Phosphonate Fragment. MD simulations of the optimized structures of native AChE and its adducts gave insight into how the skeletal motions accommodate an overcrowded active site particularly in the pentacoordinate adduct. The skeletal motions of the Cα backbone during a 120 ps molecular dynamics simulation allowed the Glu327−His440 distance to increase by ∼10% in the native AChE, which seems to give a more realistic structure of the active site. Yet the catalytic triad is tight and seems already "wound" in the reactant state to act on the substrate or inhibitor. Rmsd values and fluctuation around the average position of residues were greater in native AChE than in the covalently modified enzyme. The accommodation of the inhibitor required a substantial rearrangement at the active site and the acyl binding site, but other residues were less mobile than in the native enzyme. A full simulation may show a somewhat different picture, because residues beyond the 18 Å radius may absorb some of the skeletal rearrangement. In contrast, trypsin can accommodate the inhibitor without major changes in the mobility of the protein residues.

The H-bond distances were shortened by 0.05−0.3 Å during MD simulations in the adducts of AChE covalently modified by soman at the pentacoordinate and tetracoordinate intermediate stage (Figures 8−10) relative to the average structure of native AChE. While the stochastic boundary simulation of the adducts on the 200 ps time scale ameliorated some of the severe repulsions within the protein, it decreased the average distance between Glu199 of AChE and the pentacoordinate phosphonate fragment. Figure 6 illustrates the interaction between $HisH^+$-440 and Glu199 that occurred during MD simulation of the pentacoordinate P_RC_S diastereomer of soman-inhibited AChE. Similar tendencies can be inferred, although to a lesser extent, from the time series plots for both the penta- and tetracoordinate P_SC_S adducts of soman-inhibited AChE. Glu199 moves particularly close to the phosphonyl fragment in the tetracoordinate structures which further confirms our earlier suggestion that it has a catalytic role in the removal of the pinacolyl group in the subsequent side reaction. This *subtle reorientation of active-site residues under stress in the presence of a modifier should be relevant to the diversity and great efficiency of AChE catalysis and inhibition.*[7]

The MD calculations suggest that in AChE modified with a tetracoordinate fragment at Ser200, a small motion of the imidazole ring (15−30° rotation around Cβ-Cγ) maintained H-bonding between $HisN\delta H^+$ and Glu327 by gliding the proton from close contact with one O of the carboxylate to the other. An associated shift in the position of HisNϵ with its lone pair of electrons could enforce a concomitant proton switch from the Ser OHγ to the leaving group on the substrate. This contention is *germane to the origins of catalytic power in this evolutionarily highly developed enzyme*.

Leaving Group Departure from the Pentacoordinate Transients. An important aspect of the calculations was the promotion of leaving group departure from the pentacoordinate transient. General acid catalysis by the protonated active-site His is highly unlikely[14,45,46] in the light of the time-dependent distance between it and the leaving group in the apical position.[7b] Elimination of F^- from the apical position must be facilitated by solvation: this requirement could be met in AChE, but it seems easier at the active site of trypsin and chymotrypsin. However, active-site components in AChE that should prevail on expelling the leaving group particular in lieu of water are Glu199 providing an electrostatic "push" at ∼6 Å, aromatic residues especially Trp84 exerting compression while binding the pinacolyl group, and the oxyanion hole providing a strong positive electrostatic field that should play a role in stabilizing F^- (Figures 5 and 6). The energy barrier for F^- ion departure from the pentacoordinate transition states for phosphonylated AChE is $\Delta\Delta G^{\ddagger} = 4.5$ kcal/mol lower than that in trypsin due to these stabilizing forces.[14,15,21,47]

Reactions of some powerful organophosphorus compounds with cholinesterases most likely occur with a nearly concerted departure of the leaving group with Ser attack.[15,16,18,47] The inactivation of AChE by soman includes an induced-fit step together with the general base-catalyzed phosphonylation of the Ser.[18] A gradual adjustment may be induced as the inhibitor migrates down the active-site gorge. Conformational change was experimentally observed in the reaction of AChE with unnatural substrates,[29,30] inhibitors,[48] but not in the reaction of acetylcholine,[29,30] which occurs near the rate of diffusion.

The catalytic strategies, substrate compression, and use of the components of the catalytic apparatus thus differ between AChE and the serine proteases corresponding to their different physiological substrates. The perceptions derived from the dynamic features of AChE and its covalently modified forms broaden the scope of understanding the origins of enzyme catalytic power in general and serine hydrolase catalysis in particular.

(45) (a) Kovach, I. M.; Huhta, D.; Baptist, S. *Theochem.* **1991**, *72*, 99−110. (b) Kovach, I. M. *Theochem.* **1988**, *47*, 159−169.
(46) Kovach, I. M.; Huhta, D. *Theochem.* **1991**, *79*, 335−342.
(47) (a) Kovach, I. M.; Larson, M.; Schowen, R. L. *J. Am. Chem. Soc.* **1986**, *108*, 5490−5495. (b) Kovach, I. M.; Bennet, A. J. *Phosphorus, Sulfur and Silicon* **1990**, *51/52*, 51−56.
(48) Aslanian, D.; Grof, P.; Renault, F.; Masson, P. *Biochim. Biophys. Acta* **1995**, *1249*, 37−44.

Methods

Phosphonate Fragments. The equilibrium structures for the tetracoordinate phosphonate esters of the active-site Ser formed with soman for AChE, trypsin and chymotrypsin were reported earlier.[7] Optimized geometry and electrostatic potential (ESP)-derived partial atomic charges were generated for the pentacoordinate and tetracoordinate phosphonates in MNDO as implemented in MOPAC (6.0).[49] The geometric and charge parameters were calculated by an *ab initio* 6-31*G** basis set (GAMESS)[31] for a trigonal bipyramid, dimethoxy fluoromethylphosphonate. Using the parameters from the model compound, pentacoordinate adducts of the soman-modified Ser were generated. The charges on P were adjusted slightly according to the MNDO values. The force constants and torsional barriers for the pentacoordinate structure were obtained by analogy to parameters for similar molecular fragments and were validated by comparison to the *ab initio*-derived frequencies (6-31*G**). Force constants for the axial bonds were scaled to maintain the *ab initio* geometries.

Molecular Mechanics and Dynamics of AChE, Trypsin and Chymotrypsin and Their Soman-Inhibited Adducts. Fully refined solvated structures of the three native enzymes generated in YETI (5.3)[36] were reported previously.[7,33] The united atom representation was used in YETI. The adducts were generated by incorporating the modified Ser fragment into solvated structures of enzymes that had been energy-optimized.[7] Acidic and basic residues were given unit electrostatic charges; the effect of Glu443 on the active-site conformation was studied in the ionized and unionized form. All Tyr and Cys residues were neutral. The site of protonation of the His residues were based on the availability of H-bond donors or acceptors and were identical to those in ref 11. Both nitrogens Nϵ and Nδ were protonated on the catalytic His in all phosphonylated enzymes to correspond to the results of NMR pH-titrations of phosphorylated adducts of trypsin and chymotrypsin.[50] The enzymes thus modified with the pentacoordinate phosphonates were also optimized in YETI. The optimized structures of native AChE and trypsin were then used in 120 ps MD simulations with program CHARMM (c23f4).[32] Full-scale simulations were also carried out for 120 ps with the tetracoordinate and pentacoordinate P_SC_S diastereomer of soman-inhibited trypsin. The tetracoordinate and pentacoordinate adducts of soman-inhibited AChE were treated with the stochastic boundary method[44,51] to curtail the costs of the calculations.

CHARMM Calculations. All atoms were represented explicitly. The flexible TIP3P model was used for the simulation of a 5 Å layer of solvate water around the enzymes for full simulations.[52,53] The water−enzyme complex was energy-minimized with steepest descent and the Adapted Basis Newton-Raphson method (200 cycles each). The parameters for the amino acid residues were from the standard parameter file of the CHARMM program.[55] There was no term for H-bond in the empirical potential energy function. The temperature of the energy-minimized native AChE and trypsin were raised from 50 K to 300 K in 5 K steps in every 0.5 ps and then equilibrated for 5 ps with and 10 ps without velocity adjustment. The coordinates were saved every 0.2 ps for later analysis in 80 ps production runs at 300 K. Numerical integration by the leap frog integrator with a 1 fs step size was used for all calculations. A switching function was used on the force for the long range nonbonding energy terms with a cut-off value of 12 Å.[56]

In the stochastic boundary simulations, the system was divided into a reaction zone of 18 Å radius centered around Oγ of the active-site Ser, a 2 Å buffer shell including all residues any part of which fell within this zone and a reservoir zone.[51,54] Residues in the reservoir region were deleted except for those whose side chain reached into the buffer region. Atoms within the buffer zone were restrained by a harmonic force. The force constants were calculated for every heavy atom from the average mean-squared displacement values in the dynamics simulation of the native enzyme. The harmonic restraining force constant was multiplied by a switching function, which varied between 0 and 0.5 in the buffer region. Langevin and random forces were applied to heavy atoms in the buffer region. Heuristic update was applied to the nonbonded list, and the active zone boundary region was updated every 50 steps. The frictional coefficients were 200 ps^{-1} for the protein and 62 ps^{-1} for the water.

Additionally, pentacoordinate and tetracoordinate phosphonate esters of both diastereomers of AChE were heated to 700 K (20 K/ps), equilibrated for 20 ps at 700 K and cooled back to 300 K at a rate of 10 K/ps. The cooled structures were equilibrated at 300 K for periods of 80−120 ps. This process was carried out for two starting conformations of the P_RC_S diastereomer: in one case the phosphoryl group was placed into the oxyanion hole, and in the other the phosphoryl group was accommodated near the His440 and the methyl group was placed near the oxyanion hole while the pinacolyl group occupied the vicinity of Trp84, an optimal binding site for this bulky group, in the native AChE structure. The tetracoordinate P_SC_S diastereomer was heated to 1500 K to allow for passing even larger conformational barriers. Stochastic boundary simulations were thus carried out in duplicates. Simulated annealing was performed on an Indigo/2 Silicon Graphics workstation at CUA or on a Cray J90 supercomputer at the Pittsburgh Supercomputing Center, 200 ps stochastic boundary simulations at 300 K were either on a Cray J90 or on an HP735 cluster (NIH), and full MD simulations were on the Indigo/2 workstation and on the HP735 cluster. No discrepancy between the calculations or any artifact that may result from machine architecture were observed.

Acknowledgment. This research was supported by the National Science Foundation through Grants MCB9205927 and MCB940020P Pittsburgh Supercomputing Center. IMK gratefully acknowledges Research Fellowship 1 F33 AG05742-01 from NIA/NIH for support of her sabbatical leave. We are grateful to Dr. B. R. Brooks at NIH/DCRT for many helpful suggestions and for access to the HP 735 cluster.

JA952406V

(49) Dewar, S.; Zoebisch, E. G.; Healy, E. F.; Stewart, J. J. P. *J. Am. Chem. Soc.* **1985**, *107*, 3902−3909.

(50) Porubcan, M. A.; Westler, W. M.; Ibanez, I. B.; Markley, J. L. *Biochemistry* **1979**, *18*, 4108−4116.

(51) (a) Brooks III, C. L.; Brunger, A.; Karplus, M. *Biopolymers* **1985**, *24*, 843−865. (b) Brunger, A. T.; Brooks, C. L. III; Karplus, M. *Chem. Phys. Lett.* **1984**, *105*, 495−500. (c) Berkowitz, M.; McCammon J. A. *Chem. Phys. Lett.* **1982**, *90*, 215−217.

(52) Jorgensen, W. L.; Chandrasekhar, J.; Madura, J. D.; Impey, R. W.; Klein, M. L. *J. Chem. Phys.* **1983**, *79*, 926−935.

(53) Steinbach, P. J.; Brooks, B. R. *Proc. Natl. Acad. Sci. U.S.A.* **1993**, *90*, 9135−9139.

(54) Nakagawa, S.; Yu, H.; Karplus, M.; Umeyama, H. *Proteins: Struct. Func. Gen.* **1993**, *16*, 172−194.

(55) MacKerell Jr., A. D.; Karplus, M. unpublished.

(56) Steinbach, P. J.; Brooks, B. R. *J. Comput. Chem.* **1994**, *15*, 667−683.